Effects of edge anomaly on the appearance-potential spectroscopy of metals

Russell Patrick and Shyamalendu M. Bose
Department of Physics and Atmospheric Sciences, Drexel University, Philadelphia, Pennsylvania 19104

Pierre Longe
Institut de Physique, Batiment 5, Université de Liège, Sart-Tilman, B-4000 Liège, Belgium
(Received 17 June 1985)

The anomalous edge behavior in the appearance-potential spectroscopy of simple metals has been investigated. With the use of simple diagrams and a realistic pseudopotential for the core-hole interaction, the Nozières—De Dominicis—Laramore theory has been extended beyond the immediate neighborhood of the edge region. It is shown that close to the edge, this theory reduces to the same power-law expression as calculated by Laramore. Away from the edge, numerical results are presented for both $1s$ and $2p$ intensity spectra of Al. Derivative spectra are also calculated numerically. The resulting singularities and widths of the edge structures in both $1s$ and $2p$ derivative spectra are consistent with experimental data.

I. INTRODUCTION

The anomalous edge behavior in the x-ray band spectra of metals was first investigated by Mahan[1] and Anderson.[2] The singularities at the edge in the emission (absorption) -intensity spectra are due to the interaction of the core hole with the conduction band. The first process contributing to the edge behavior, known as the orthogonality catastrophe, creates low-energy particle-hole pairs because of the change in potential due to the sudden destruction (creation) of a core hole as seen by the conduction band. The core hole is assumed to have no recoil (e.g., infinite effective mass) and therefore can excite an enormous number of particle-hole pairs with little expenditure of energy. The departure (intrusion) of an electron in the conduction band also affects this edge behavior. This second process deals with the interaction between the core hole and the additional hole (electron) in the conduction band and was first related by Mahan to the excitonic scattering in semiconductors. These two competing processes were combined in the Nozières—De Dominicis (ND) theory,[3] which relates the scattering of the conduction electrons due to the sudden change in potential in terms of their phase shifts (δ_l) near the Fermi surface. The ND theory is a one-body theory, where one looks at the response of each conduction electron to the sudden change in potential due to the destruction (creation) of a core hole. The form for the x-ray-emission (absorption) intensity near the edge is given by a power law

$$I_l(\omega)=I_0(\omega)G_0\left[\frac{\xi_0}{|\omega-\varepsilon_F|}\right]^{\alpha_l} \tag{1}$$

with

$$\alpha_l=\frac{2\delta_l}{\pi}-2\sum_{l'=0}^{\infty}(2l'+1)\left[\frac{\delta_{l'}}{\pi}\right]^2, \tag{2}$$

where $I_0(\omega)$ is the one-electron transition intensity and ε_F is the Fermi energy. G_0 and ξ_0 are constants on the order of 1 and ε_F, respectively. The first power term is related to the open-line part of the ND theory (rearrangement term), while the second is due to the closed-loop part of the ND theory (Anderson catastrophe). Note that the sign of α_l given in (2) determines if the intensity at the edge is convergent or divergent.

The ND theory was applied to the appearance-potential spectra (APS) of metals by Laramore.[4] In the APS experiment, a solid surface is bombarded by a fast electron (energy ε_k), which excites a core electron (energy E_B) and thus in the final state, the system contains a core hole and two electrons above the Fermi level. Experimentally, what is measured is the x-ray-emission intensity (deexcitation of the core hole) as a function of the incident energy. The threshold (edge) region of the spectrum corresponds to both final-state electrons being very close to the Fermi surface. Laramore gives a power-law expression near the APS edge which can be expressed as

$$I_l(\varepsilon_k)\sim\left[\frac{\xi_0}{\varepsilon_k-E_B-2\varepsilon_F}\right]^{\gamma_l} \tag{3}$$

with exponent

$$\gamma_l=\frac{4\delta_l}{\pi}-2\sum_{l'=0}^{\infty}(2l'+1)\left[\frac{\delta_{l'}}{\pi}\right]^2-1\ . \tag{4}$$

The additional factor of 2 in the first term of the exponent γ_l appears because APS results in two final-state electrons causing the scattering, and the additional -1 in γ_l is due to the self-convolution in the zeroth-order process (no effective interaction).

Another two-electron process, the Auger process, was also studied in the framework of the ND theory by Natta and Joyes (NJ).[5] In Auger spectroscopy, one electron of an electron pair in the conduction band falls into the pre-

viously created core hole, while the other is ejected as an "Auger" electron. A power law similar to the APS form was found. The ND theory was also applied to the photoemission spectra by Doniach and Sunjic (DS).[6]

The edge theory described so far is reliable only at energies close to the threshold. The theory was extended to regions away from the edge in the x-ray-emission and absorption spectra of metals by one of the authors (P.L.).[7] Unlike the other theories which require that a separable scattering potential be used, the Longe theory allows the use of a *realistic* nonseparable potential, which is an essential requirement in dealing with regions away from the edge. The extended theory essentially results in replacement of the constants G_0 and ξ_0 in (1) by energy-dependent values $G_0(\omega)$ and $\xi_0(\omega)$. The extended theory was later applied to the Auger spectra of metals by Longe and Bose (LB).[8] Using this extended theory, they found a shift in the position of the maximum of the Auger spectrum. In this paper we follow the method of LB to study the effect of the sudden creation of the core hole on the APS process and thereby obtain a measure of the width and strength of the edge structure.

In Sec. II we give a general formulation of the APS problem in terms of a Hamiltonian describing the process, and introduce the pseudopotential used to describe scattering of the conduction electrons by the core hole. The APS process is then related to "one-body"—type diagrams which can be separated into "closed-loop" (orthogonality catastrophe) and "open-line" (excitonic process) diagrams. In Secs. III and IV the closed-loop and open-line parts are calculated to obtain the intensity in terms of the phase shifts. Numerical results for both the $1s$ and $2p$ APS intensity spectra of Al and their derivative spectra are given in Sec. V. The derivative spectra are also observed in APS experiments as they enhance any structures that may be present (edge, plasmon satellites, etc.) in the intensity spectra. As in the experimental data, the calculated intensity spectra at the edge will be shown to be convergent while the derivative spectra divergent.

II. FORMALISM

Our model for the metal consists of a filled conduction band up to the Fermi level and deep core levels that are recoilless (can absorb infinite momentum). We also assume that the core hole cannot change its state, i.e., there is no finite lifetime of the hole due to Auger-type transitions. The purpose for these assumptions is to have a hole lifetime long enough so that the conduction-band electrons have enough time to adjust to the hole potential.[9] This structureless hole is what gives rise to the abrupt edge effect. The zero of the energy levels is taken to be at the bottom of the conduction band so that the core-level energies are negative.

The Hamiltonian describing the APS process can be written as

$$H = H_0 + H_{\text{el-}B} + H_{kB} \tag{5a}$$

with

$$H_0 = \sum_{p\,(<k_F)} \varepsilon_p a_p^\dagger a_p + E_B a_B^\dagger a_B + \varepsilon_k a_k^\dagger a_k \ , \tag{5b}$$

$$H_{\text{el-}B} = \sum_{\substack{p'\,(<k_F),\\ p\,(>k_F)}} V(p,p') a_p^\dagger a_{p'} a_B a_B^\dagger \ , \tag{5c}$$

$$H_{kB} = \sum_{\substack{p\,(>k_F),\\ p'\,(>k_F)}} W_{kpp'} a_p^\dagger a_{p'}^\dagger a_k a_B \ . \tag{5d}$$

H_0 describes the noninteracting system where we have a filled conduction band (energy states $\varepsilon_p = p^2 < \varepsilon_F$) and filled core level with energy E_B (<0). (In this paper we will take $2m = \hbar = 1$.)

The second term in the Hamiltonian, $H_{\text{el-}B}$, is the interaction term between the final-state core hole and the conduction electrons which is responsible for the edge behavior. $V(p,p')$ is the potential seen by the conduction electrons and is written as

$$V(p,p') = V(q) = \frac{V_{\text{ps}}(q)}{\epsilon(q)} \ , \tag{6}$$

where $q = |\mathbf{p} - \mathbf{p}'|$, $\epsilon(q)$ is the static Lindhard dielectric function describing the polarization of the conduction band, and V_{ps} is the Coulomb pseudopotential containing the information about the size and strength of the scatterer (core hole). The formalism presented in this paper uses the Ashcroft pseudopotential,[10] which is Coulombic outside a cutoff radius R_c and zero inside R_c. The original Ashcroft radius will be modified, using a proportionality rule introduced by Longe,[7] to take into account the effect of the missing core electron. In momentum space this pseudopotential takes the form

$$V_{\text{ps}} = \frac{4\pi e^2}{q^2} \cos(qR_c^*) \ , \tag{7}$$

where R_c^* is the cutoff radius modified by the absence of a core electron. Note that this potential, unlike the ones used in other edge theories, is nonseparable.

The last Hamiltonian term H_{kB} is the interaction Hamiltonian describing the creation of the core hole by the incident electron with energy ε_k. Since our energy region of interest is small ($\approx \varepsilon_F$ away from the threshold), the transition matrix element ($W_{kpp'}$) which has been shown elsewhere[11,12] to have small variation for small momentum transfers, will be considered a constant, c.

Since the object of this study is to find the edge shape of the APS intensity spectrum, interaction effects among conduction electrons which give a smooth background to the spectrum, along with any plasmon structures at higher energies,[12,13] is not considered.

In the APS process, the initial state (ϕ) is a filled conduction band and an incident electron with energy ε_k with no core holes. In the final state, there is a core hole and two electrons are present above the Fermi level. The intensity can be written in terms of the linear-response function as

$$I(\omega) = \frac{1}{\pi} \operatorname{Re} \int_0^\infty ds\, e^{i\omega s} F(s) \ , \tag{8}$$

where

$$\omega = \varepsilon_k + E_B \ ,$$

and

$$F(s)=\frac{\langle\phi\,|\,U(\infty,s)H_{kB}(s)U(s,0)H_{kB}(0)U(0,-\infty)\,|\,\phi\rangle}{\langle\phi\,|\,U(\infty,-\infty)\,|\,\phi\rangle} \tag{9}$$

is the response function in the interaction picture. The interaction Hamiltonian acts between times 0 and s. U is the time-development operator and the denominator in (9) corresponds to the S matrix.

The Feynman diagrams showing the APS process in the zeroth, first, and a typical seventh order are given in Fig. 1. The corresponding "one-body" graphs used by ND are given in Fig. 2 where the open circles represent the initiation of the APS process (removal of a core electron by the bombarding electron). For an nth-order interaction process there are n solid circles. Those attached to the single line pointing up represent scattering of the final-state electrons above the Fermi level by the core hole. Solid circles on the closed loops represent particle-hole pair creation due to the core-hole interaction with the conduction band. Comparing the full Feynman diagrams (Fig. 1) and the "one-body" diagrams (Fig. 2), we note that for each "one-body" diagram there are three Feynman diagrams; two diagrams to include both spin states (contributing a factor of 2) and one exchange diagram (contributing a factor of -1).

A calculation of the zeroth-order intensity (no effective interaction) is now carried out by applying the diagrammatic rules, stated in the Appendix, to Fig. 2(a). The total response function is

$$F^{(0)}(s)=\left[c^2\int_{k_F}^{\infty}dp_1p_1^2e^{-ip_1^2s}\right]\times\left[c^2\int_{k_F}^{\infty}dp_2p_2^2e^{-ip_2^2s}\right]. \tag{10}$$

Inserting this response function into the intensity expression (8) and performing the s integration we obtain

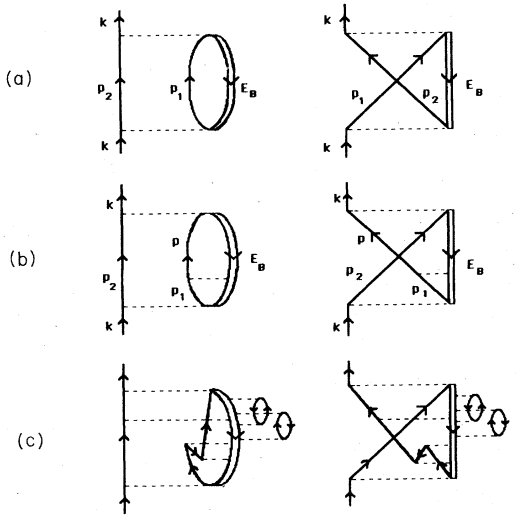

FIG. 1. Feynman diagrams (direct and exchange) describing the APS process in the (a) zeroth, (b) first, and (c) a typical seventh order. A single line pointing up (down) represents a particle (hole) above (below) the Fermi level. A double line pointing down represents a core hole, while a dashed-horizontal line represents the static Coulomb interaction.

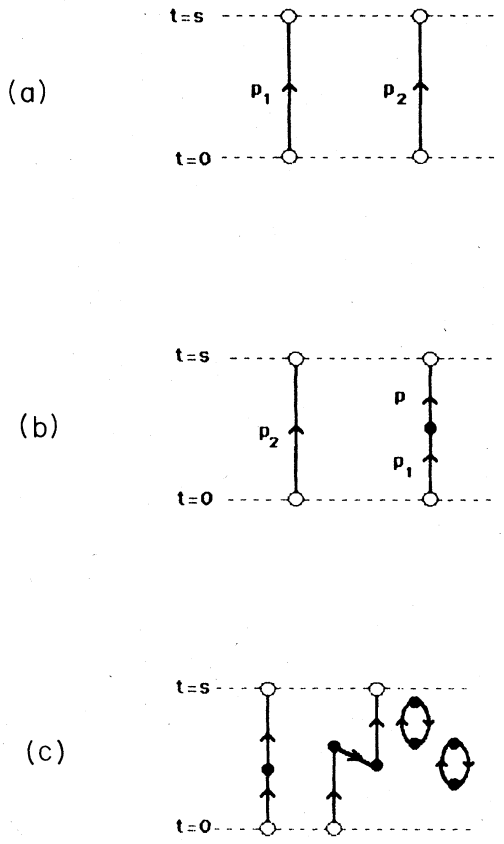

FIG. 2. Diagrammatic representation in the manner of Nozières and De Dominicis of the APS process in the (a) zeroth, (b) first, and (c) a typical seventh order. The open circles represent the interaction of the incident electron with a core state, while the solid circles represent scattering by the core hole.

$$I_0(\omega)=\frac{c^4}{4}\int_{\varepsilon_F}^{\infty}d\varepsilon_{p_1}\int_{\varepsilon_F}^{\infty}d\varepsilon_{p_2}\delta(\omega-\varepsilon_{p_1}-\varepsilon_{p_2})(\varepsilon_{p_1}\varepsilon_{p_2})^{1/2} \tag{11a}$$

$$=\frac{c^4}{4}\left[\left[\frac{\omega-2\varepsilon_F}{2}\right][\epsilon_F(\omega-\varepsilon_F)]^{1/2}+\left[\frac{\omega}{2}\right]^2\sin^{-1}\left[1-\frac{2\varepsilon_F}{\omega}\right]\right]\Theta(\omega-2\varepsilon_F)\,, \tag{11b}$$

where Θ is the step function. The term $(\varepsilon)^{1/2}$ is the free-electron density of states and (11a) is just the self-convolution of the density of states. Near the edge, the density of states can be replaced by a constant $(\epsilon_F)^{1/2}$ and an approximate form to (11a) can be given as

$$I_0^0(\omega\sim2\varepsilon_F)=\frac{c^4}{4}\varepsilon_F(\omega-2\varepsilon_F)\Theta(\omega-2\varepsilon_F)\,. \tag{12}$$

As discussed in Ref. 8, the correlation function $F(s)$ can be expressed as the product

$$F(s)=F_{\rm op}(s)F_c(s)\ , \tag{13}$$

where $F_{\rm op}(s)$ and $F_c(s)$ correspond to the open-line part and closed-loop part of the APS problem, respectively. In the next two sections we describe the methods of calculating $F_c(s)$ and $F_{\rm op}(s)$, and their contributions to the intensity of the APS spectra of simple metals are calculated by using (8).

III. CLOSED-LOOP PART

The purpose of this section is to calculate all contributions from the closed-loop diagrams, which describe both the scattering of conduction-band electrons by the core hole (between times $t=0$ and $t=s$) and the vacuum polarization part (S matrix). Our final result for the intensity function due to the closed loops $[I_c(\omega)]$ will then be cast in a form similar to Laramore's (3), but the function ξ_0 will now be energy dependent. Using the linked-cluster theorem, the closed-loop part of the response function can be written as

$$F_c(s)=e^{[C(s)-C(0)]}\ , \tag{14}$$

where $C(s)$ is the contribution of all single-loop terms and $C(0)$ corresponds to the contribution of the S matrix. In this article we will only use the two-vertex loop, the first nonzero contribution to $C(s)$. (The one-vertex loop is the Hartree term, which is canceled out by the positive-ion background of the electron gas.) As was explained in Refs. 7 and 8, this corresponds to calculating the scattering process in the Born approximation. Furthermore, $F_c(s)$ will first be calculated from

$$F_c(s)\approx 1+C_2(s)-C_2(0)\ , \tag{15}$$

which is the expansion of (14) retaining up to first-order terms. Its contribution to the intensity function will subsequently be recast in the exponential form[7,8] as discussed below. Using the diagrammatic rules stated in the Appendix, one obtains

$$C_2(s)-C_2(0)=-2\sum_{l'=0}^{\infty}(2l'+1)\int_{k_F}^{\infty}dp\int_0^{k_F}dq\,p^2(-q^2)[iD_l(p,q)]^2\int_0^s dt_1\int_{t_1}^s dt_2\,e^{i(p^2-q^2)(t_1-t_2)}\ . \tag{16}$$

Information about the phase shifts is included in

$$\sigma(p,q)=-\frac{pq}{2}\sum_{l'=0}^{\infty}(2l'+1)[D_l(p,q)]^2\ . \tag{17}$$

Since we are dealing with plane waves, (17) may be written in the following integral form:

$$\sigma(p,q)=-\frac{1}{(2\pi)^4}\int_{|p-q|}^{p+q}dk\,k[V(k)]^2 \tag{18}$$

with $V(k)$ given by (6). After performing the t and t' integrations function (16) becomes

$$C_2(s)-C_2(0)=\int_{k_F}^{\infty}dp\int_0^{k_F}dq\frac{4pq}{(p^2-q^2)^2}\sigma(p,q)\times(1-e^{-i(p^2-q^2)s})\ . \tag{19}$$

A term proportional to is has been dropped because its effect when put back into the exponential form (14) is only to shift the whole spectrum uniformly, which is irrelevant to the present problem. Substitutions of (19) into (15), of (15) into (13) and of (13) into (8) and subsequent evaluation of the s integral yields

$$I(\omega)=I_{\rm op}(\omega)[1+Z(\omega)]\ , \tag{20}$$

where

$$Z(\omega)=\int_{k_F}^{\infty}dp\int_0^{k_F}dq\frac{4pq}{(p^2-q^2)^2}\sigma(p,q)\times\left[1-\frac{I_0^0(\omega-p^2+q^2)}{I_0^0(\omega)}\right]\ . \tag{21}$$

Note that in the bracketed term in (21) we have replaced the open-line intensity function $I_{\rm op}(\omega)$, by the zeroth-order function near the edge (12). This approximation is made in $Z(\omega)$ to avoid complications introduced by higher-order corrections which have negligible contributions.[8] Once $Z(\omega)$ is calculated, the closed-loop part intensity function is recast in the exponential form

$$I_c(\omega)=e^{Z(\omega)}\ , \tag{22}$$

as was done in Refs. 7 and 8. As mentioned above, this in a sense corresponds to evaluation of $I_c(\omega)$ using (14) for $F_c(s)$ rather than (15). Placing (12) into (21) we have for the $Z(\omega)$ term

$$Z(\omega)=\int_A dp\,dq\frac{4pq\sigma(p,q)}{(p^2-q^2)^2}+\frac{1}{(\omega-2\varepsilon_F)}\int_a dp\,dq\frac{4pq\sigma(p,q)}{(p^2-q^2)}\ , \tag{23}$$

where the regions of integration a and A are shown in Fig. 3. Since the integrands are ill-behaved as p approaches q, let us recast (23) into the following form:

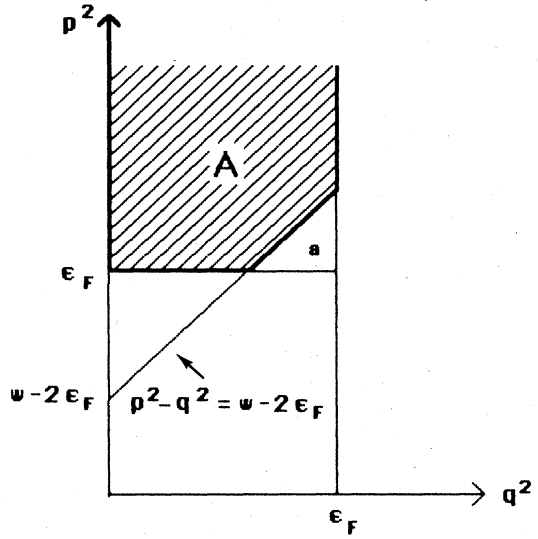

FIG. 3. Regions of integration (a and A) for the evaluation of the closed-loop function $Z(\omega)$ by (24). Note that the shape of each region changes for $\omega > 3\varepsilon_F$.

$$Z(\omega)=\sigma_{00}\left[\int_A \frac{dp^2dq^2}{(p^2-q^2)^2}+\frac{1}{(\omega-2\varepsilon_F)}\int_a \frac{dp^2dq^2}{p^2-q^2}\right] + \int_A \frac{dp^2dq^2}{(p^2-q^2)^2}[\sigma(p,q)-\sigma_{00}] + \frac{1}{(\omega-2\varepsilon_F)}\int_a \frac{dp^2dq^2}{p^2-q^2}[\sigma(p,q)-\sigma_{00}] , \tag{24}$$

where

$$\sigma_{00}=\sigma(k_F,k_F) . \tag{25}$$

Each integrand in (24) is now well behaved, and the separation of terms allows us to factor out a power-law term while the remainder is a smooth function of ω. The integrations in the first two terms in (24) have been performed analytically with the result

$$Z(\omega)=\sigma_{00}\mathcal{L}(\omega)+\sigma_{00}^{*}\ln\left|\frac{\varepsilon_F}{\omega-2\varepsilon_F}\right| , \tag{26}$$

where

$$\sigma_{00}\mathcal{L}(\omega)=2\sigma_{00}^{*}+\int_A \frac{dp^2dq^2}{(p^2-q^2)^2}[\sigma(p,q)-\sigma_{00}] + \frac{1}{(\omega-2\varepsilon_F)}\int_a \frac{dp^1dq^2}{p^2-q^2}[\sigma(p,q)-\sigma_{00}] \tag{27}$$

and

$$\sigma_{00}^{*}=\sigma_{00}\left[\Theta(3\varepsilon_F-\omega)+\Theta(\omega-3\varepsilon_F)\left[\frac{\varepsilon_F}{\omega-2\varepsilon_F}\right]\right] . \tag{28}$$

The total intensity function from the closed-loop contribution, from (26) and (22), is now

$$I_c(\omega)=e^{\sigma_{00}\mathcal{L}(\omega)}\left[\frac{\varepsilon_F}{\omega-2\varepsilon_F}\right]^{\sigma_{00}^{*}} . \tag{29}$$

We obtain a one-to-one correspondence of (29) to Laramore's closed-loop part result[4] if we allow ω to approach $2\varepsilon_F$ and if we define the finite constant $e^{\sigma_{00}\mathcal{L}(\varepsilon_F)}$ by ξ_0:

$$I_c(\omega\sim 2\varepsilon_F)=e^{\sigma_{00}\mathcal{L}(2\varepsilon_F)}\left[\frac{\varepsilon_F}{\omega-2\varepsilon_F}\right]^{\sigma_{00}} . \tag{30}$$

III. OPEN-LINE PART

As shown in Fig. 2, the open-line part of the APS process can be regarded as the self-convolution of two x-ray-absorption lines $I_x(\omega)$

$$I_o(\omega)=\int_{\varepsilon_F}^{\infty} d\varepsilon_{p_1}\int_{\varepsilon_F}^{\infty} d\varepsilon_{p_2} I_x(\varepsilon_{p_1})I_x(\varepsilon_{p_2}) \times\delta(\omega-\varepsilon_{p_1}-\varepsilon_{p_2}) . \tag{31}$$

Note that the substitution

$$I_x^0(\varepsilon)=\frac{c^2}{2}\sqrt{\varepsilon} \tag{32}$$

gives us the zero-order spectra [Eq. (11)]. To calculate the APS spectrum to all orders, (1) will be used for each x-ray line, but away from the edge (Ref. 7) both G_0 and ξ_0 will have an ω dependence. In addition, only the $l=0$ component of the phase shift in the exponent will be used. The validity of this approximation has been discussed in Ref. 8.

Our new x-ray-absorption line will now be written as

$$I_x(\omega)=\frac{c^2}{2}\sqrt{\omega}G_0(\omega)\left[\frac{\xi_0(\omega)}{\omega-\varepsilon_F}\right]^{2\delta_0/\pi} . \tag{33}$$

The procedure for calculating the open-line power law is similar to that for the closed-loop part, except for the additional $G_0(\omega)$ factor. $G_0(\omega)$ is a consequence of having two different scattering vertices (open and solid circles), each having a different momentum dependence

The calculation of $G_0(\omega)$ and $\xi_0(\omega)$ are given in Ref. 7, where it is shown that $\xi_0(\omega)$ is a slowly varying function of ω with a limiting value $\xi_0(\varepsilon_F)=\varepsilon_F$, and $G_0(\omega)$ is also a smooth function of ω except at the Fermi edge (ε_F), where it approaches 1 with an infinite slope[14] i.e.,

$$G_0(\varepsilon_F)=1, \quad \left.\frac{dG_0(\omega)}{d\omega}\right|_{\omega=\varepsilon_F}=\infty . \tag{34}$$

The forms for $G_0(\omega)$ and $\xi_0(\omega)$ given in Ref. 7 by Eqs. (53) and (21), respectively, have been used in our calculation.

Using the delta function to perform the ε_{p_2} integration in (31) and introducing in the remaining integral the dimensionless variable

$$x=\frac{\varepsilon_{p_1}-\varepsilon_F}{\omega-2\varepsilon_F} , \tag{35}$$

we obtain

$$I_{\rm op}(\omega)=\frac{c^4}{4}(\omega-2\varepsilon_F)^{1-4\delta_0/\pi}\int_0^1 dx\frac{1}{[x(1-x)]^{1-4\delta_0/\pi}}$$
$$\times\{g[(\omega-2\varepsilon_F)x+\varepsilon_F]g[(\omega-2\varepsilon_F)(1-x)+\varepsilon_F]\}\ , \tag{36}$$

where

$$g(y)=\sqrt{y}\,[\xi_0(y)]^{2\delta_0/\pi}G_0(y)\ . \tag{37}$$

A numerical integration of this is prohibitive since the integrand diverges at the endpoints. With some simple algebraic manipulations, however, we can recast (36) into

$$I_{\rm op}(\omega)=\frac{c^4}{4}(\omega-2\varepsilon_F)^{1-4\delta_0/\pi}\left[\frac{2^{2\delta_0/\pi}}{(1-2\delta_0/\pi)}g(\varepsilon_F)g(\omega-\varepsilon_F)\right.$$
$$+\int_0^{1/2}\frac{dx}{x^{2\delta_0/\pi}}\left[\frac{g[(\omega-2\varepsilon_F)x+\varepsilon_F]g[(\omega-2\varepsilon_F)(1-x)+\varepsilon_F]}{(1-x)^{2\delta_0/\pi}}-g(\varepsilon_F)g(\omega-\varepsilon_F)\right]$$
$$\left.+\int_{1/2}^1\frac{dx}{(1-x)^{2\delta_0/\pi}}\left[\frac{g[(\omega-2\varepsilon_F)x+\varepsilon_F]g[(\omega-2\varepsilon_F)(1-x)+\varepsilon_F]}{x^{2\delta_0/\pi}}-g(\varepsilon_F)g(\omega-\varepsilon_F)\right]\right]. \tag{38}$$

The integral in (38) can be carried out numerically.

This function corresponds to the open-line part of Laramore's result (3) if we set $\xi_0(y)=\varepsilon_F$ and $G_0(y)=1$, which is valid in the edge region $\omega\sim 2\varepsilon_F$. The resulting integral can be done analytically with the result

$$I_{\rm op}(\omega\sim 2\varepsilon_F)\sim\frac{c^4}{4}\varepsilon_F(\varepsilon_F e^{L_0})^{4\delta_0/\pi}$$
$$\times\frac{[\Gamma(1-2\delta_0/\pi)]^2}{\Gamma(1-4\delta_0/\pi)}(\omega-2\varepsilon_F)^{1-4\delta_0/\pi}\ , \tag{39}$$

where

$$L_0=1+\int_{k_F}^{\infty}dp\int_0^{k_F}dq\frac{4pq}{(p^2-q^2)^2}\left[\frac{\sigma_0(p,q)}{\sigma_0(k_F,k_F)}-1\right] \tag{40}$$

with

$$\sigma_0(p,q)=-\frac{pq}{2}[D_0(p,q)]^2\ .$$

V. RESULTS AND DISCUSSION

The total intensity function may now be written as the product of intensities due to the closed-loop part (29) and the open-line part (38) as

$$I(\omega)=I_c(\omega)I_{\rm op}(\omega)$$
$$=\frac{c^4}{4}\Theta(\omega-2\varepsilon_F)\frac{(\varepsilon_F e^{L(\omega)})^{\sigma_{00}}}{(\omega-2\varepsilon_F)^{4\delta_0/\pi+\sigma_{00}^*-1}}\left[\frac{2^{2\delta_0/\pi}}{(1-2\delta_0/\pi)}g(\varepsilon_F)g(\omega-\varepsilon_F)\right.$$
$$+\int_0^{1/2}\frac{dx}{x^{2\delta_0/\pi}}\left[\frac{g[(\omega-2\varepsilon_F)x+\varepsilon_F]g[(\omega-2\varepsilon_F)(1-x)+\varepsilon_F]}{(1-x)^{2\delta_0/\pi}}\right.$$
$$\left.-g(\varepsilon_F)g(\omega-2\varepsilon_F)\right]$$
$$\left.+\int_{1/2}^1\frac{dx}{(1-x)^{2\delta_0/\pi}}\left[\frac{g[(\omega-2\varepsilon_F)x+\varepsilon_F]g[(\omega-2\varepsilon_F)(1-x)+\varepsilon_F]}{x^{2\delta_0/\pi}}\right.\right.$$
$$\left.\left.-g(\varepsilon_F)g(\omega-2\varepsilon_F)\right]\right]. \tag{41}$$

This function gives a measure of the effect of low-energy electron-hole pair creation on the APS of metals. Before proceeding with the numerical calculation of (41) away from the edge, let us note that close to the edge, (41) reduces to [see (30) and (39)]

$$I(\omega\sim 2\varepsilon_F)=\frac{c^4}{4}\Theta(\omega-2\varepsilon_F)\varepsilon_F(\varepsilon_F e^{L_0})^{4\delta_0/\pi}(\varepsilon_F e^{L_0})^{\sigma_{00}}\frac{[\Gamma(1-2\delta_0/\pi)]^2}{\Gamma(1-4\delta_0/\pi)}(\omega-2\varepsilon_F)^{-(4\delta_0/\pi+\sigma_{00}-1)}, \tag{42}$$

which has the same power-law behavior and energy dependence as (3) or Eq. (17) in Ref. 4.

Numerical calculation of (41) has been carried out for the $1s$ and $2p$ APS spectra and their derivatives for Al (radius parameter $r_s/a_0=2.07$). As mentioned in Sec. II, the cutoff radius R_c in the pseudopotential (7) has been modified to take into account the effect of the missing core electron using a proportionality rule (Ref. 7)

$$\frac{R_c^*}{R_c}=\frac{R_{\rm SL}^*}{R_{\rm SL}}. \tag{43}$$

In this equation, R_c is the cutoff radius for a free atom, $R_{\rm SL}$ is the radius of the valence electrons obtained by using Slater rules,[15] and $R_{\rm SL}^*$ is the Slater radius with the missing core electron. For Al, $R_c=0.59$ Å, $R_{\rm SL}=0.453$ Å, $R_{\rm SL}^*=0.365$ Å for an L-shell electron missing, and $R_{\rm SL}^*=0.353$ Å for a K-shell electron missing. The proportionality rule gives $R_c^*=0.475$ Å and $R_c^*=459$ Å for the L and K shells, respectively. The phase shifts were calculated in the Born approximation at the Fermi level. As mentioned in Sec. III, only s-wave scattering is considered for the open-line part. The values for δ_0 are 0.407 for the $2p$ spectrum and 0.428 for the $1s$ spectrum.

The calculated APS spectra for the $1s$ and $2p$ excitations in Al are shown in Fig. 4 along with the one-electron band shape (dashed line). Since both spectra have negative power-law exponents, they are finite but have a large positive slope at the edge. The derivative spectra calculated numerically are shown in Fig. 5. Near the edge both the $1s$ and $2p$ derivative spectra are divergent, with a strong negative slope. Away from the edge, however, the derivative spectra are slowly varying with a positive slope. The dashed curve in Fig. 5 corresponds to the derivative one-electron spectrum of Al.

It is interesting to attempt to compare our results with the currently available experimental APS spectra of Al. Andersson and Nyberg[16] have measured the $1s$ APS spectrum and Nilsson and Kanski[17] have measured the $2p$ spectrum. The various structures appearing in the experimental spectra are the effects of superposition of the many-body effects (edge anomaly, plasmon and single-pair excitations, etc.) and the band-structure effects. Since we have not included the band-structure effects in our calculation it is not possible to make a quantitative comparison of our results with experiment. Nonetheless, we notice that the threshold peaks calculated in this paper are very similar to the ones observed experimentally in the $1s$ and $2p$ derivative APS spectra. A comparison of the two observed spectra indicates that the $1s$ spectrum is more sharply peaked at the threshold—a conclusion borne out by our theoretical calculation. The sharpness of these peaks is not as great in the experimental spectra because the hole has some structure. However, the experimental $1s$ spectrum exhibits more of the singular nature of the theoretical line shape. This is not surprising in that the $1s$ spectrum is better suited for comparison with any "one-body" theory since the $1s$ core hole ($E_B=-1547$ eV) has less mobility than the $2p$ core hole ($E_B=-61.4$ eV). Nyberg and Andersson have concluded from the analysis of their experimental data that the width of the threshold

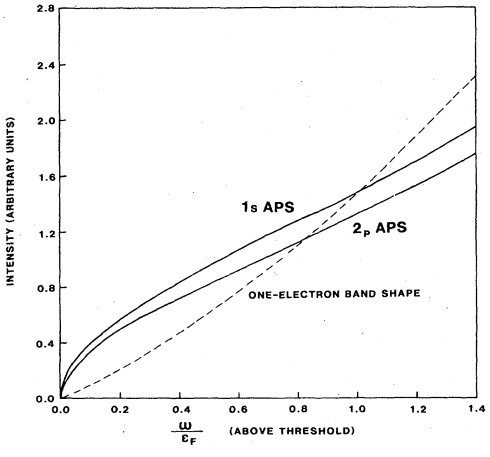

FIG. 4. Line shapes for the $1s$ and $2p$ APS of Al. The dashed line represents the one-electron band shape, which is proportional to the self-convolution of the density of states.

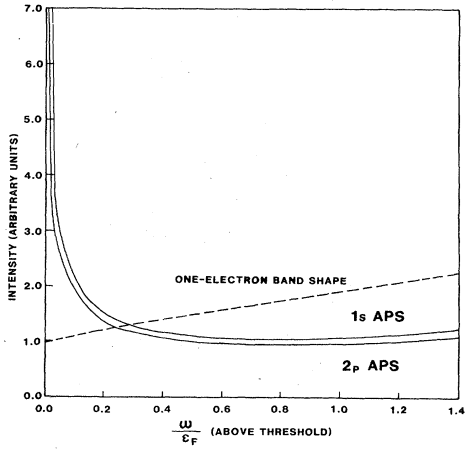

FIG. 5. Derivative spectra of the $1s$ and $2p$ APS of Al. The dashed line represents the derivative of the one-electron band shape.

peak of the $1s$ spectrum is approximately 0.95 eV. Our calculated spectra appear to be wider. However, for a quantitative comparison with experiment one must include other many-body effects and band-structure effects in the theoretical calculation.

Finally, in this paper we have calculated the many-body effects of the sudden creation of the core hole on the edge structure of the APS spectra of Al. By using a realistic nonseparable potential for the scattering of the conduction electrons by the core hole, we have been able to extend the calculation beyond the intermediate neighborhood of the edge region. Our theory results in large peaks in the derivative APS spectra and shows that, unlike the x-ray-absorption and emission cases, both $1s$ and $2p$ derivative spectra have singularities in the edge region verifying experimental observations. Our calculation also corroborates the experimental fact that the edge structure in the $1s$ derivative spectrum is more sharply peaked than the $2p$ derivative spectrum.

ACKNOWLEDGMENTS

One of the authors (PL) is grateful to Fonds National de la Recherche Scientifique, Belgium and the Coopération Scientifique Internationale, Belgium, for financial support.

APPENDIX: DIAGRAMMATIC RULES

The rules for calculating the diagrams which describe the response function $F(s)$ are as follows.

(a) For an open circle, which describes the creation of a core hole, a constant c. This is a constant since we are assuming a constant transition matrix element $W_{kpp'}$.

(b) For each solid circle a factor of $iD_l(p,q)$, the core-vertex function. This function comes from the core-hole scattering matrix element

$$\int d\mathbf{x}\,\bar{\psi}_p(\mathbf{x})V(r)\psi_q(\mathbf{x}) , \tag{A1}$$

where the ψ_k's are the conduction-electron wave functions. Since the conduction electrons are described by plane waves, the angular part is separable and (A1) can be written as

$$\sum_{l=0}^{\infty}\sum_{m=-l}^{l}\bar{Y}_l^m(\hat{\mathbf{p}})Y_l^m(\hat{\mathbf{q}})D_l(p,q) , \tag{A2}$$

where

$$D_l(p,q)=\frac{2}{\pi}\int dr\, r^2 j_l(pr)V(r)j_l(qr) , \tag{A3}$$

or as an integration over k, $D_l(p,q)$ is[7]

$$D_l(p,q)=\frac{1}{4\pi^2 pq}\int_{|p-q|}^{p+q} dk\, kV(k)P_l\left[\frac{p^2+q^2-k^2}{2pq}\right] .$$

Note that this is related to the Born approximation if we set $p=q$. Scattering will occur near the Fermi level, so the Born approximation is made for the lth phase shift

$$\delta_l=\frac{\pi}{2}k_F D_l(k_F,k_F) . \tag{A4}$$

(c) For each particle line (arrow pointing up) of momentum p between times t_1 and t_2, a factor $p^2e^{ip^2}(t_1-t_2)\Theta(p-k_F)$, where Θ is the unit step function.

(d) For each hole line (arrow pointing down) of momentum q between times t_1 and t_2, a factor $-q^2e^{iq^2}(t_1-t_2)\Theta(k_F-q)$.

(e) Include a factor $-2(2l+1)$ for each closed loop.

(f) Sum over all angular momentum quantum numbers l.

(g) Integrate over all internal momenta and times.

[1]G. D. Mahan,Phys. Rev. **163**, 612 (1967).
[2]P. W. Anderson, Phys. Rev. Lett. **18**, 1049 (1967).
[3]P. Nozières and C. T. De Dominicis, Phys. Rev. **178**, 1097 (1969).
[4]G. E. Laramore, Phys. Rev. Lett. **27**, 1050 (1971).
[5]M. Natta and P. Joyes, J. Chem. Phys. Chem. Solids **31**, 447 (1970).
[6]S. Doniach and M. Šunjić, J. Phys. C **3**, 285 (1970).
[7]P. Longe, Phys. Rev. B **8**, 2572 (1973).
[8]P. Longe and S. M. Bose, Phys. Rev. B **19**, 1905 (1979).
[9]K. D. Schotte and U. Schotte, Phys. Rev. **185**, 509 (1969).
[10]N. W. Ashcroft, Phys. Lett. **23**, 48 (1966); J. Phys. C **1**, 232 (1968).
[11]J. J. Chang and D. C. Langreth, Phys. Rev. B **5**, 3512 (1972).
[12]G. E. Laramore, Solid State Commun. **10**, 85 (1972).
[13]R. Patrick, S. M. Bose, and P. Longe, Phys. Rev. B **32**, 3507 (1985).
[14]P. Longe, Phys. Rev. B **10**, 529 (1974).
[15]J. C. Slater, Phys. Rev. **36**, 57 (1930).
[16]A. Andersson and C. Nyberg, Solid State Commun. **28**, 803 (1978).
[17]P. O. Nilsson and J. Kanski, Surf. Sci. **37**, 700 (1973).